Soil Biology and Biochemistry 166 (2022) 108564

Contents lists available at ScienceDirect

Soil Biology and Biochemistry

journal homepage: www.elsevier.com/locate/soilbio

Contrasting effects of straw and biochar on microscale heterogeneity of soil O_2 and pH: Implication for N_2O emissions

Kun Zhu [a], Xin Ye [a], Hongyu Ran [a], Peixuan Zhang [a,b], Gang Wang [a,*]

[a] Department of Soil and Water Sciences, China Agricultural University, Yuanmingyuan West Road 2, Haidian District, Beijing, 100193, China
[b] School of Engineering, Westlake University, Hangzhou, Zhejiang, China

ARTICLE INFO

Keywords:
Oxygen and pH dynamics
Straw-soil interfaces
Straw derived biochar
Planar optode
N_2O emission

ABSTRACT

Little is known about the microscale heterogeneity of O_2 and pH in the interfaces between soil and amendments. In this study, planar optodes were applied to continuously measure the micro-scale O_2 and pH dynamics in soil amended with a patch of straw and its biochar. The recalcitrant biochar with high porosity had stronger capability to maintain the oxic zone around the patch area. Mainly through diffusion of alkali carbonates, the biochar increased the soil pH within a few hours but in constrained area (<4.5 mm from the surface of the biochar patch). Such high pH coupled with oxic conditions largely restricted N_2O emissions in the biochar treatment. The sufficient labile carbon from straw induced fast O_2 consumption with microoxic development in the straw-soil interfaces, while its porous structure could enhance O_2 diffusive inputs in the core area, therefore, the microoxic area was formed as a concentric ring around the straw patch. Such enriched oxic-microoxic transient zones would induce nitrification coupled denitrification, which led to the high N_2O emissions. Additionally, the microbial degradation of straw resulted in a pulse decline of soil pH, which possibly inhibited the N_2O reductases, consequently enhanced N_2O emissions. Those results demonstrate the contrasting effects of straw and straw derived biochar on microscale O_2 and pH localization as well as the associated N_2O emissions. It will contribute to a better understanding of the driving factors for N transformations on a microscale and has the potential to become valuable tool in environmental monitoring.

Returning crop residue to soil is a common practice to maintain soil quality and improve carbon (C) sequestration in soil (Shen et al., 2014; Zhang et al., 2019). However, it has frequently been criticized due to its potential to enhance greenhouse gas (GHG) emissions from soils. One alternative approach, incorporating straw derived biochar to the soil, has already drawn extensive attentions (Palansooriya et al., 2019). As an organic amendment in soil, biochar could significantly impact the N turnover and mitigate N_2O emissions from soil (Lehmann and Joseph, 2015). One of those promising mechanisms that might explain N_2O variations is soil aeration and pH dynamics influenced by straw/biochar application (Russenes et al., 2016). The interfaces between straw/biochar and soil particles are acknowledged as key hotspots for the GHG productions and emissions (Lehmann et al., 2015), however, very few studies have examined quantitively the spatial and temporal O_2 and pH dynamics within such interfaces, which might lead to a very patchy distribution of the major N transformation processes that contribute to N_2O emissions. The objective of this study was to investigate the microscale heterogeneity of O_2 and pH distributions along the soil – straw/biochar interfaces, as well as their implications for N_2O emissions.

The sandy loam soil used in this study had organic C content 8.8 g kg^{-1}, total N 0.8 g kg^{-1} and pH 7.4 (1:2.5, soil/water). The maize straw contained 44.3% C and 0.5% N. The biochar was obtained through pyrolysis of the maize straw at 500 °C, which had a pH of 10.1 (1:20, soil/water) and contained 65.1% C and 0.5% N. The plastic petri dishes were used as the soil containers and equipped with semi-transparent planar optode sensor on the bottom. The petri dish was packed with soil (37.0 g dry soil with a depth of 12 mm, a diameter of 55 mm) to reach a bulk density of 1.30 Mg m^{-3}. Soil was pre-incubation under 50% of the water holding capacity for one week prior to the experiment. Then it was wetted with deionised water to 85% of the water holding capacity. The petri dish was covered by plastic film to reduce the soil water evaporation, and maintain the oxygen exchange between the soil headspace and air with several holes in the covered film. One control (CON, no amendment), one straw amended treatment (ST) and one biochar amended treatment (BC) using the same application rate (1.0 g DM kg^{-1} dry soil) were established.

* Corresponding author. Yuanmingyuan West Road 2, Haidian District, Beijing, 100193, China.
E-mail address: gangwang@cau.edu.cn (G. Wang).

https://doi.org/10.1016/j.soilbio.2022.108564
Received 25 July 2021; Received in revised form 20 October 2021; Accepted 15 January 2022
Available online 17 January 2022

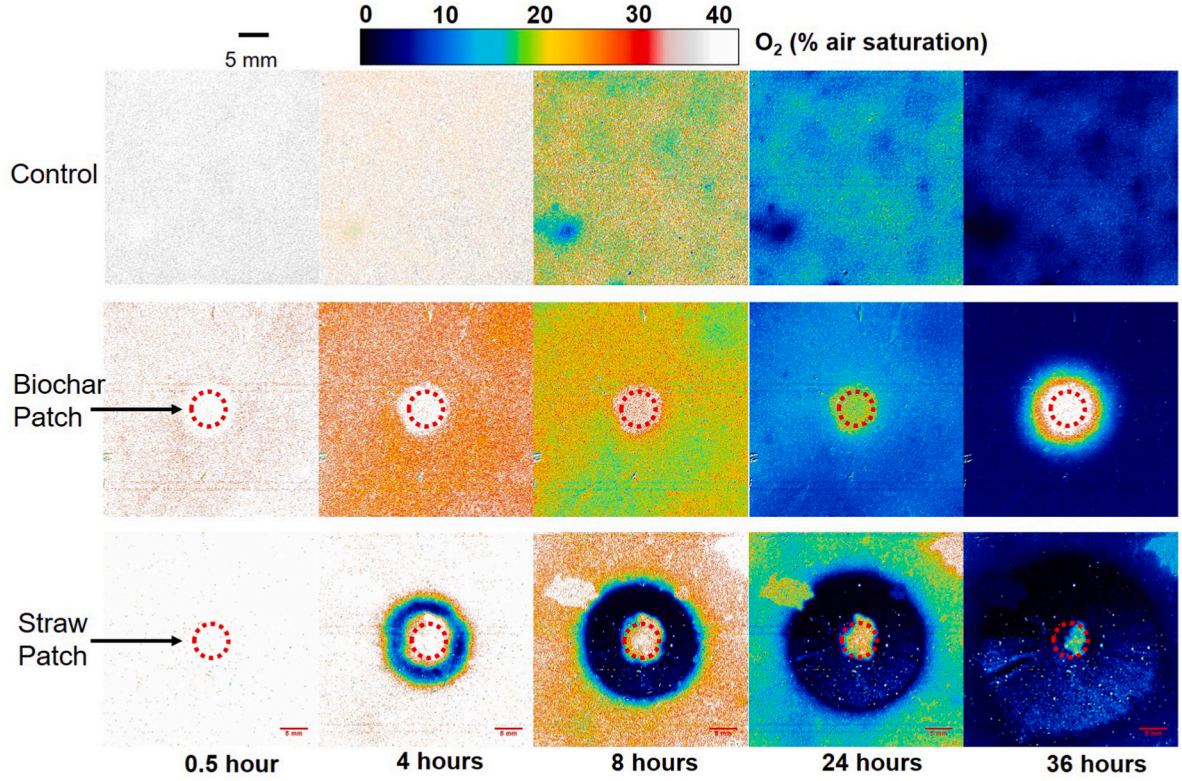

Fig. 1. Soil O_2 dynamics after the application of straw and straw derived biochar patch. The red dotted circles indicated the locations of the biochar/straw patch. Images are one representative example of the three replicates. The other two replicates were shown in Fig. S2. (For interpretation of the references to colour in this figure legend, the reader is referred to the Web version of this article.)

The straw/biochar amended treatments were constructed by placing the amendments (straw or biochar) as a cylindric patch (diameter of 5 mm) in the center of soil mesocosm. Since only three treatments could be monitored at the same time in our optode system, six trials were conducted sequentially (CON, ST and BC in triplicates): three trials for monitoring O_2 dynamics, the other three for pH measurement. All trials were monitored for 36 h under room temperature of 21 ± 2 °C and air humidity of 40–60%. An additional set of incubation petri dishes were

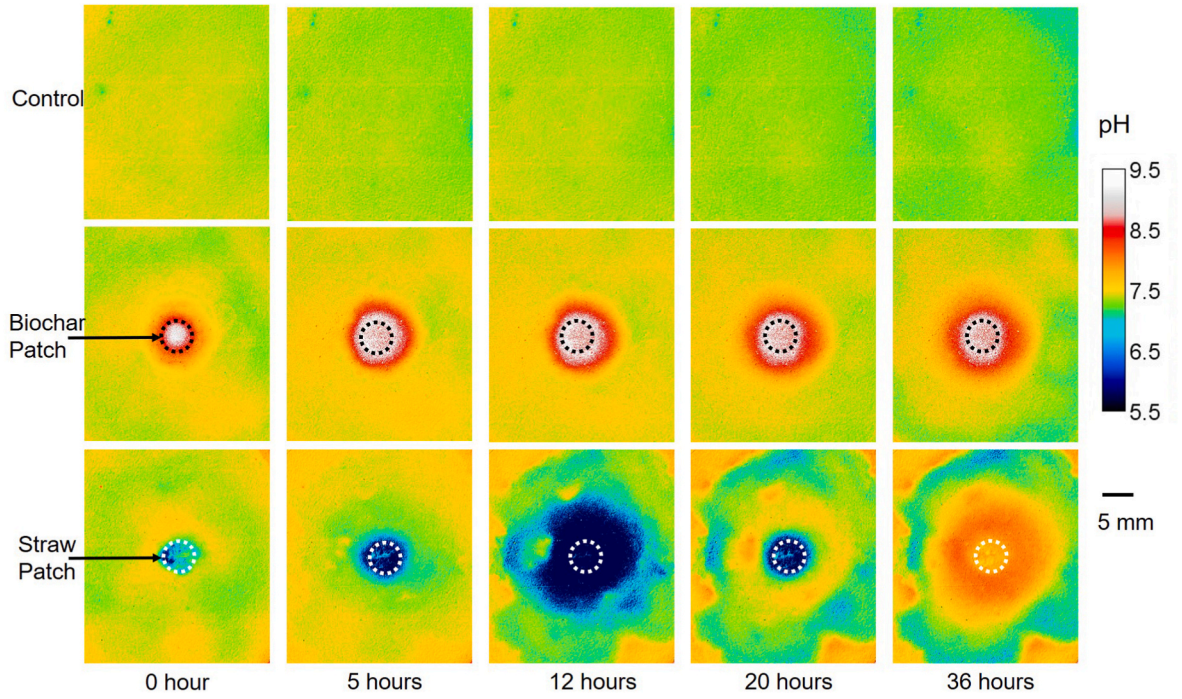

Fig. 2. Selected images of pH distribution in soil after application straw or straw derived biochar. Images are one representative example of the three replicates. The other two replicates were shown in Fig. S3. The black and white dotted circles are the locations of biochar and straw patch respectively.

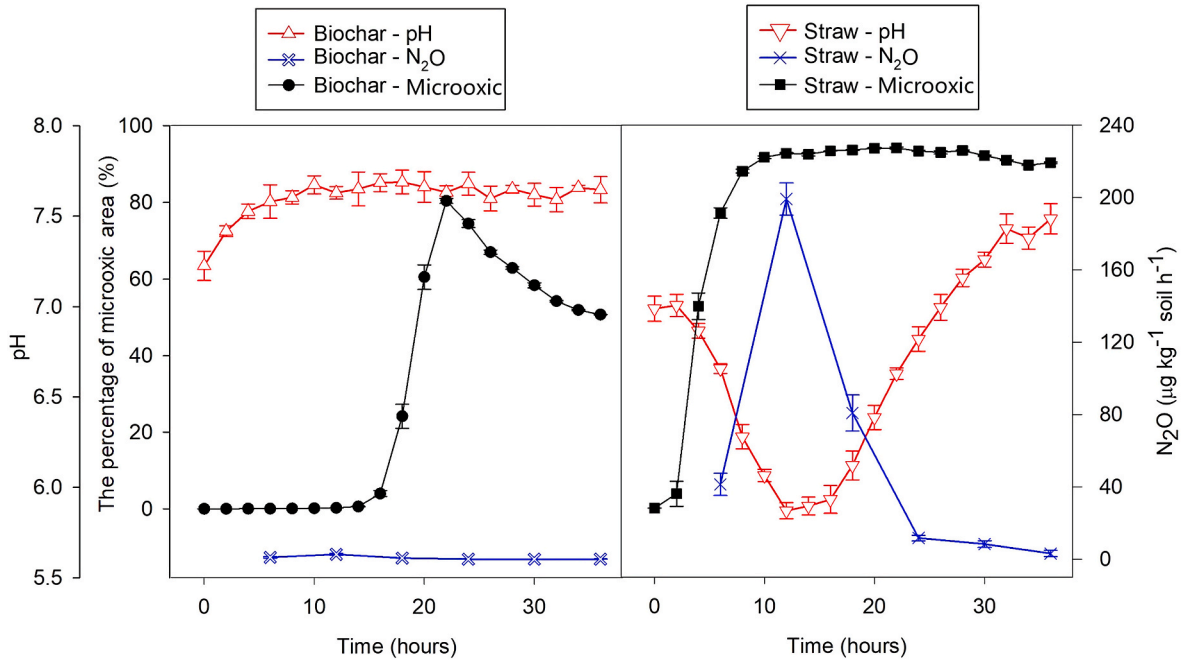

Fig. 3. The percentage of micooxic area, mean soil pH (calculated from the selected soil area displayed in Figs. 1 and 2) and N_2O emission rates in biochar and straw patch treatments.

prepared for the gas measurements every 6 h. Gas sampling was performed by placing each petri dish in an airtight 1.5 L plastic box. At each sampling event, 20 mL gas was taken using a 50-mL gas-tight syringe from the headspace of the plastic box after 0 and 6 h. The concentrations of N_2O were measured using gas chromatograph (Agilent 7890A, Agilent Ltd., Shanghai, China).

The applied planar optode set-up was adapted from Larsen et al. (2011). Briefly, the O_2 specific planar optode is a sensor with a luminescent indicator Pt(II)-tetrakis(pentafluorophenyl)porphyrin (PtTFPP). The excitation light (550 nm) was used to emit a characteristic luminescence depending on the O_2 contents. The pH specific planar optode is a sensor with a luminescent indicator 5-hexadecanoylaminofluorescein, which after light excitation (405 nm) emits a characteristic luminescence depending on the pH values. The pH optode membrane was directly coated on the bottom of petri dishes. The O_2 optode membrane was coated on a glass (36 mm × 36 mm), which was inserted in the bottom of the customized dishes, the same size as the petri dishes used for pH monitoring (Fig. S1). A Canon EOS 760D camera was used to record the luminescent signals from the optode sensors. The recorded images were processed using the software ImageJ (http://rsbweb.nih.gov/ij/).

The straw and straw derived biochar significantly influenced the spatial distributions of soil O_2 dynamics. With straw degradation, the soil O_2 was consumed fast in the interfaces of straw and soil. The percentage of microoxic area (O_2 content < 5% air saturation) (Keiluweit et al., 2018) in straw treatment was sharply increased after 4 h, and reached over 90% at the end of experiment. The products from the straw degradation would diffuse to the surrounding soil zones, offering sufficient C sources for the microbial activities, consequently enhanced the soil O_2 consumption, and the microoxic zone was formed as a concentric ring around the straw patch (Fig. 1). In the core of the straw patch, the O_2 contents were depleted in a relatively slower rate. This is possibly due to the higher porosity in the straw patch, which facilitated the O_2 inputs (diffusion from the headspace air). The higher N_2O emission from straw treatment was closely linked with the soil microoxic area as well as the transient microoxic - oxic zones around the straw patch. The fast development of microoxic area (in the concentric ring) favored the denitrification, while the transient microoxic - oxic zones (the boundaries of concentric ring) would possibly induce the occurrence of nitrification coupled denitrification. Both processes could contribute to the high N_2O emissions from straw treatment.

While in the biochar treatment, the O_2 content in the biochar patch decreased in the initial period, and then rose up to 30% air saturation. Most of the biochar C was recalcitrant, however, there were limited contents of labile C from biochar, which could be available for microbial activities, hence induce a slight decline of soil O_2 initially. In the later stage, the porous structure of biochar was beneficial for the O_2 diffusion, therefore, the O_2 inputs into the biochar patch would be much higher than that in the surrounding soil. The percentage of microoxic area was negligible in the initial 16 h. Such enhanced soil aeration in biochar patch would largely restricted N_2O emissions.

Both biochar and straw patch had significant impacts on spatio-temporal variations of soil pH (Fig. 2). Particularly, a very quick pH elevation was observed in the biochar patch area. The biochar influencing area extended to a distance of 4.5 mm beyond the patch boundary after 36 h, which was 1.8 times of the biochar patch radius. Those pH changes were probably contributed from the readily released alkaline substances of biochar (Yuan et al., 2011), particularly the inorganic carbonates (0.32% of carbonate-C in biochar used in this study). At the location >5.0 mm from the biochar patch boundary, the pH was not significantly changed at all, indicating that the biochar influences on soil pH was limited in local zones (Buss et al., 2018). The influencing area of the biochar patch would be constrained mainly by two factors: the acid-base buffering capacity of soil and the alkalinity of biochar (Fidel et al., 2017). Those two factors mostly determined the alkalis diffusions and consumption in the biochar-soil interfaces. Additionally, water movement caused by rainfall or irrigation in the soil may also be a factor affecting the influencing area of biochar amendments. Furthermore, the biochar's effects on soil microbial processes (i.e., N_2O formation) would always be limited in such localized spots, namely charosphere. As the oxic zones in charosphere would constrain the denitrification, coupling with the elevated soil pH that would favour the reductase activities of N_2O, the N_2O emissions were greatly reduced in the biochar treatment (Cayuela et al., 2014; Obia et al., 2015).

Contrasting to biochar, the effect of straw patch on soil pH displayed with a significantly different pattern. During the first 15 h of the

experiment, straw patch decreased the pH by 1.5 unit in the patch center, extending to a distance of ~12.5 mm, 5 times of the straw patch radius. After this pH descending period, the pH of the straw patch increased gradually and reached to a pH value of 8.0 at the end of the experiment. The pH in the earlier acidified soil area had been increased as well. There were several pathways responsible for those soil pH changes: in the early stage, the direct contribution of acidic organic compounds contained in the straw would initially decrease the soil pH. Furthermore, the degradation of straw-derived DOC under O_2-limited conditions (Fig. 1) could produce various types of organic acids (Song et al., 2014), which are highly mobile in soil and are capable to acidify the surrounding soils. Therefore, it decreased the soil pH rapidly over a relatively wide area. Such pH decline may inhibit the N_2O reductase activities, therefore, the occurrence of low pH spots, coupled with the fast development of microoxic area, could contribute to the hot moment of N_2O emission right after straw addition (Fig. 3) (Shaaban et al., 2018).

Our optode study showed that application of straw and biochar differentially influenced the heterogeneity of O_2 and pH zonation in soil-straw and soil-biochar interfaces. Such O_2 and pH variations had controlling influences on the production patterns of N_2O. These results are highly relevant for defining the size of different microbial hot spots and understanding microbial driven processes in soils. Further experiments coupled with measurements on the gradients of substrate and microbial functions, such as diffusive gradients in thin films (Lehto et al., 2017), zymography (Ma et al., 2019), will be able to further shed light on O_2 and pH - regulated N_2O productions.

Declaration of competing interest

The authors declare that they have no known competing financial interests or personal relationships that could have appeared to influence the work reported in this paper.

Acknowledgements

This study was supported by the National Natural Science Foundation of China (grant number 42177311) and the National Key Research and Development Program of China (grant number 2017YFD0200801-02).

Appendix A. Supplementary data

Supplementary data to this article can be found online at https://doi.org/10.1016/j.soilbio.2022.108564.

References

Buss, W., Shepherd, J.G., Heal, K.V., Mašek, O., 2018. Spatial and temporal microscale pH change at the soil-biochar interface. Geoderma 331, 50–52.
Cayuela, M.L., van Zwieten, L., Singh, B.P., Jeffery, S., Roig, A., Sánchez-Monedero, M. A., 2014. Biochar's role in mitigating soil nitrous oxide emissions: a review and meta-analysis. Agriculture, Ecosystems & Environment 191, 5–16.
Fidel, R.B., Laird, D.A., Thompson, M.L., Lawrinenko, M., 2017. Characterization and quantification of biochar alkalinity. Chemosphere 167, 367–373.
Keiluweit, M., Gee, K., Denney, A., Fendorf, S., 2018. Anoxic microsites in upland soils dominantly controlled by clay content. Soil Biology and Biochemistry 118, 42–50.
Larsen, M., Borisov, S.M., Grunwald, B., Klimant, I., Glud, R.N., 2011. A simple and inexpensive high resolution color ratiometric planar optode imaging approach: application to oxygen and pH sensing. Limnology and Oceanography: Methods 9, 348–360.
Lehmann, J., Joseph, S., 2015. Biochar for Environmental Management: Science and Technology, second ed. Earthscan, London, UK.
Lehmann, J., Kuzyakov, Y., Pan, G., Ok, Y.S., 2015. Biochars and the plant-soil interface. Plant and Soil 395, 1–5.
Lehto, N.J., Larsen, M., Zhang, H., Glud, R.N., Davison, W., 2017. A mesocosm study of oxygen and trace metal dynamics in sediment microniches of reactive organic material. Scientific Reports 7, 11369.
Ma, X., Mason-Jones, K., Liu, Y., Blagodatskaya, E., Kuzyakov, Y., Guber, A., Dippold, M. A., Razavi, B.S., 2019. Coupling zymography with pH mapping reveals a shift in lupine phosphorus acquisition strategy driven by cluster roots. Soil Biology and Biochemistry 135, 420–428.
Obia, A., Cornelissen, G., Mulder, J., Dörsch, P., 2015. Effect of soil pH increase by biochar on NO, N2O and N2 production during denitrification in acid soils. PLoS One 10, e0138781.
Palansooriya, K.N., Ok, Y.S., Awad, Y.M., Lee, S.S., Sung, J.-K., Koutsospyros, A., Moon, D.H., 2019. Impacts of biochar application on upland agriculture: a review. Journal of Environmental Management 234, 52–64.
Russenes, A.L., Korsaeth, A., Bakken, L.R., Dörsch, P., 2016. Spatial variation in soil pH controls off-season N2O emission in an agricultural soil. Soil Biology and Biochemistry 99, 36–46.
Shaaban, M., Wu, Y., Khalid, M.S., Peng, Q.-a., Xu, X., Wu, L., Younas, A., Bashir, S., Mo, Y., Lin, S., Zafar-ul-Hye, M., Abid, M., Hu, R., 2018. Reduction in soil N2O emissions by pH manipulation and enhanced nosZ gene transcription under different water regimes. Environmental Pollution 235, 625–631.
Shen, J., Tang, H., Liu, J., Wang, C., Li, Y., Ge, T., Jones, D.L., Wu, J., 2014. Contrasting effects of straw and straw-derived biochar amendments on greenhouse gas emissions within double rice cropping systems. Agriculture, Ecosystems & Environment 188, 264–274.
Song, Z., Yang, Gaihe, Liu, X., Yan, Z., Yuan, Y., Liao, Y., 2014. Comparison of seven chemical pretreatments of corn straw for improving methane yield by anaerobic digestion. PLoS One 9, e93801.
Yuan, J.-H., Xu, R.-K., Zhang, H., 2011. The forms of alkalis in the biochar produced from crop residues at different temperatures. Bioresource Technology 102, 3488–3497.
Zhang, J., Wei, Y., Liu, J., Yuan, J., Liang, Y., Ren, J., Cai, H., 2019. Effects of maize straw and its biochar application on organic and humic carbon in water-stable aggregates of a Mollisol in Northeast China: a five-year field experiment. Soil and Tillage Research 190, 1–9.